Evolution of ASC Immunophenotypical Subsets During Expansion In Vitro

Peng, Qiuyue; Alipour, Hiva; Porsborg, Simone; Fink, Trine; Zachar, Vladimir

Published in:
International Journal of Molecular Sciences

DOI (link to publication from Publisher):
10.3390/ijms21041408

Publication date:
2020

Document Version
Publisher's PDF, also known as Version of record

International Journal of
Molecular Sciences

MDPI

Article

Evolution of ASC Immunophenotypical Subsets During Expansion In Vitro

Qiuyue Peng, Hiva Alipour, Simone Porsborg, Trine Fink and Vladimir Zachar *

Department of Health Science and Technology, Regenerative Medicine Group, Aalborg University, Fredrik Bajers Vej 3B, 9220 Aalborg, Denmark; qp@hst.aau.dk (Q.P.); hiva@hst.aau.dk (H.A.); sriis@hst.aau.dk (S.P.); trinef@hst.aau.dk (T.F.)

* Correspondence: vlaz@hst.aau.dk

Received: 29 January 2020; Accepted: 17 February 2020; Published: 19 February 2020

Abstract: Adipose-derived stromal/stem cells (ASCs) are currently being considered for clinical use for a number of indications. In order to develop standardized clinical protocols, it is paramount to have a full characterization of the stem cell preparations. The surface marker expression of ASCs has previously been characterized in multiple studies. However, most of these studies have provided a cross-sectional description of ASCs in either earlier or later passages. In this study, we evaluate the dynamic changes of 15 different surface molecules during culture. Using multichromatic flow cytometry, ASCs from three different donors each in passages 1, 2, 4, 6, and 8 were analyzed for their co-expression of markers associated with mesenchymal stem cells, wound healing, immune regulation, ASC markers, and differentiation capacity, respectively. We confirmed that at an early stage, ASC displayed a high heterogeneity with a plethora of subpopulations, which by culturing became more homogeneous. After a few passages, virtually all ASCs expressed CD29, CD166 and CD201, in addition to canonical markers CD73, CD90, and CD105. However, even at passage 8, there were several predominant lineages that differed with respect to the expression of CD34, CD200 and CD271. Although the significance of remaining subpopulations still needs to be elucidated, our results underscore the necessity to fully characterize ASCs prior to clinical use.

Keywords: adipose-derived stem cells; immunophenotype; co-expression; subpopulations; regenerative medicine

1. Introduction

Adipose-derived stromal/stem cells (ASCs) are a favorable type of mesenchymal stem cell (MSC) due to easy accessibility, high cell yield, and robust proliferative capacity [1,2]. ASCs have been recognized to be highly biologically active, with regenerative roles in tissue formation, homeostasis, and immune regulation [3–5]. These unique properties render ASCs attractive in scenarios where the traditional approaches fall short of the desired therapeutic outcome, such as for chronic wounds, diabetic ulcers, osteoarthritis, ischemic heart disease, or type 1 diabetes, just to mention a few important areas [6–10]. Many ASC-based regimens have already progressed into clinical testing, and in the United States alone, more than 20 phase I and II clinical trials are currently being conducted (clinicaltrials.gov). All of the protocols are based on the use of crude ASC cultures, which are heterogeneous mixtures containing various stem and progenitor cells that differ functionally and immunophenotypically. Additionally, the properties and ratios of these subpopulations have been shown to change along with in vitro expansion [11]. It is unlikely that all lineages within the cell preparation participate to the same extent in the therapeutic effect [12]. Provided that the discrete subpopulations can be linked with particular functionalities, it would be possible in the prospective cell-based protocols to tailor the desired properties to the clinical application, which would undoubtedly benefit the clinical outcome.

The analysis of surface epitope expression is a powerful tool to identify and isolate stem cells. Initially, in addition to plastic adherence and capacity for tri-lineage differentiation, a very specific triad of cluster of differentiation (CD) molecules CD73, CD90, and CD105 was claimed to represent the quintessential ASC hallmark [13]. However, the ensuing research lacks consensus in regard to the full stem cell marker profile of ASCs [1,14–16]. Additionally, many other molecules have been reported in association with ASCs, but their expression still remains controversial and is believed to be affected by donor-to-donor variability, differing protocols of isolation and expansion, and diverse experimental techniques [17–22]. In addition to investigations aiming at the descriptive characterization of the surface marker expression, a great effort was dedicated to elucidating the relationship between the phenotypical features and the functional properties. Indeed, some phenotypes displaying specific patterns of positivity and negativity for a limited number of selected markers have been found to possess an enhanced functionality, such as increased differentiation potential, pro-angiogenic effect, and higher proliferative rate or modulation of the immune response [15,23–29].

In our previous work, while looking at six CD markers, we demonstrated that only 8% of all possible combinations were present [12]. Thus, it is plausible that the heterogeneity of ASC cultures is limited with only a restricted number of variants, depending on the permissive combinations of the CD markers. To shed more light on the possible combinatorial repertoires, we, in the current study, based on a thorough literature search, highly expanded the number of membrane molecules to 15 markers and examined their triple co-expression according to functional grouping into 5 categories, including MSC markers, wound healing, immune regulation, ASC markers, and differentiation capacity [24,25,27–45]. This was done in the search for better insight into the dynamic changes of the immunophenotypical subsets and to elucidate the significance of the choice of donor and the effect of culture expansion. We found that at an early stage, ASCs displayed a high heterogeneity with a plethora of subpopulations, which by culturing became homogenized due to three ways of re-distribution: exchange, converge, or diverge. This was independent of the choice of donor; however, donor-dependent differences in the dynamic of some ASC subsets were discovered.

2. Results

2.1. Temporal Changes of ASC Surface Markers during In Vitro Expansion

Stromal vascular fractions (SVF) from the three donors were seeded and expanded at standard cell culture conditions for 8 passages (P) with an average of 1.76 population doublings per passage. The cultures underwent the most dramatic morphological changes during the first expansion, where the cells evolved from pleiomorphic appearance to more uniform, fibroblast-resembling types in the early P1 (Figure 1).

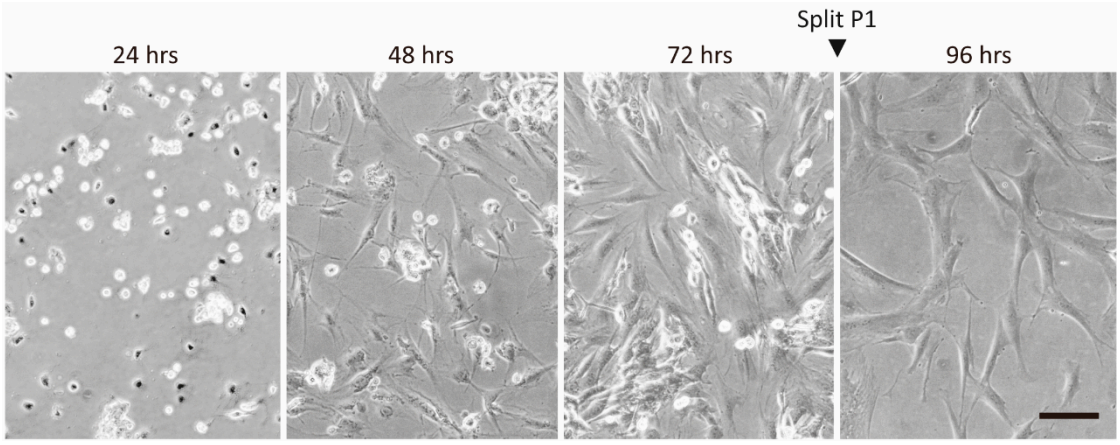

Figure 1. Development of adipose-derived stromal/stem cell (ASC) morphology after isolation (P0), and establishment of passage 1 (P1). Original magnification 200×. Scale bar indicates 100 µm.

To study the immunophenotypical changes of ASCs during the expansion period, 15 markers, including CD73, CD90, CD105, CD248, CD200, CD201, CD36, CD274, CD29, CD166, CD34, CD146, CD31, CD27, and the Stro-1, were selected based on their relevance for ASCs and their proposed functionality. For the analysis, the markers were sorted by function into five panels: MSC markers, wound healing, immune regulation, ASC markers, and differentiation capacity (Table 1). Each panel thus consisted of three markers, which were then assayed simultaneously using multi-color flow cytometry. This setup enabled the follow-up of expressional kinetics of individual markers as well as the evolution of more complex co-expressional patterns.

Table 1. Panel design for flow cytometry.

Panels					Cytometer Setup		
1. MSC Markers	**2. Wound Healing**	**3. Immune Regulation**	**4. ASC Marker**	**5. Differentiation Capacity**	**Laser**	**Emission Channel**	**Fluorochrome**
CD105	CD166	CD29	CD146	CD201	405 nm	450/45BP	BV421
						525/40BP	BV510
				CD36		610/20BP	BV605
						660/20BP	BV650
FVS570	FVS570	FVS570	FVS570	FVS570	561 nm	610/20BP	PE-CF594
	CD271	CD200	CD34			585/42BP	Viability dye
						780/60BP	PE-Cy7
	CD248	CD274	CD31	Stro-1	638 nm	660/20BP	AF647
						712/25BP	APC-R700
						780/60BP	APC-Cy7
CD73					488 nm	525/40BP	FITC
CD90						690/50BP	PerCP-Cy5.5

ASC; adipose-derived stromal/stem cells, MSC; mesenchymal stem cell,, BP; band pass, FVS570; fixable viability stain 570, AF647; Alexa Fluor 647.

When looking at the expression of single markers, only the integrin β-1 (CD29; Panel 3) was consistently expressed, irrespective of the culture period (Figure 2). Not surprisingly, the MSC prototypical markers from Panel 1 stabilized with culture time, but the CD166 and CD201 from Panels 2 and 5, respectively, also followed this pattern. The ASC markers in Panel 4 generally diminished during the culture, whereas the markers associated with wound healing (Panel 2), immune regulation (Panel 3), and differentiation (Panel 5) remained expressed at variable levels throughout the culture period.

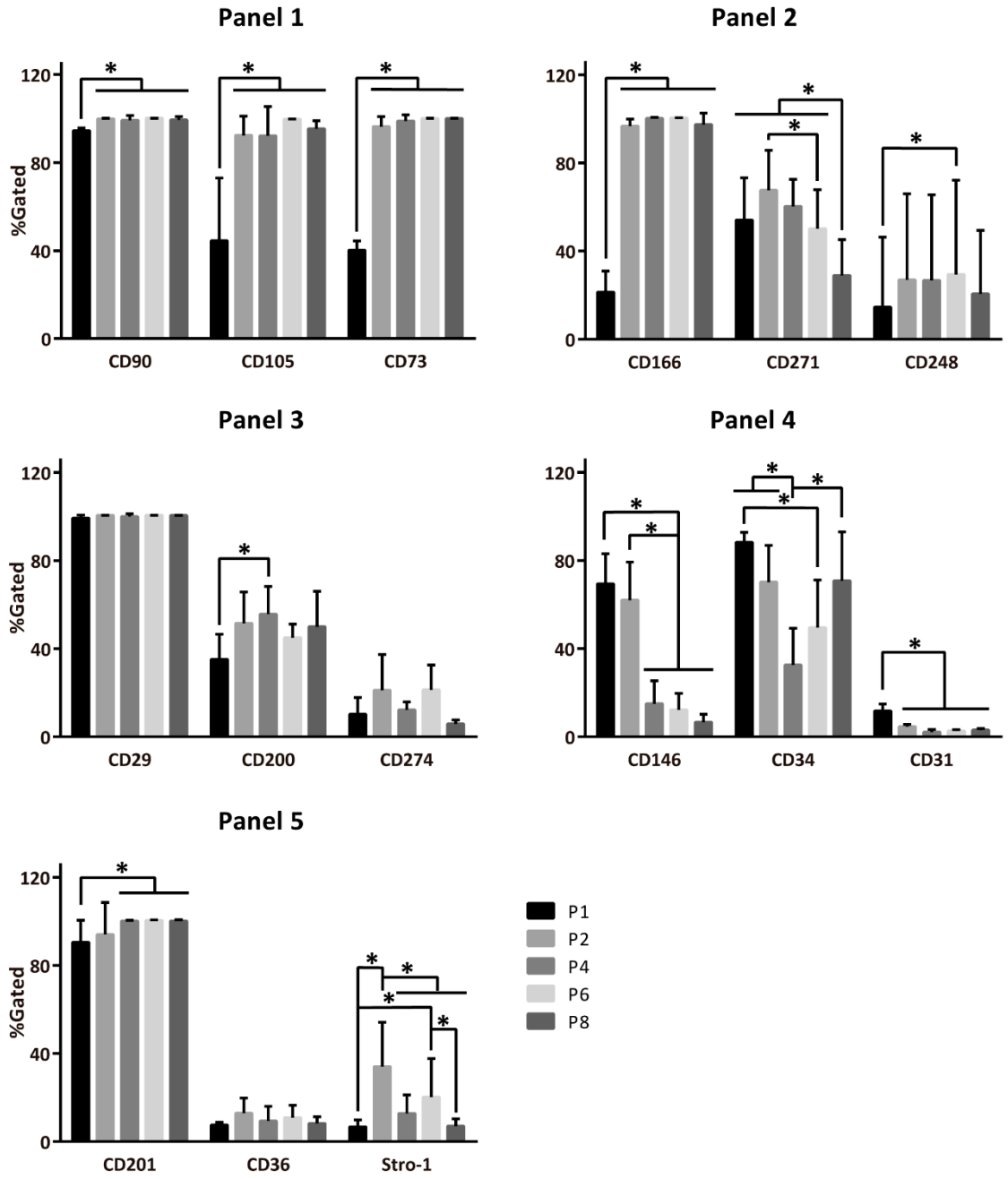

Figure 2. Development of single-marker expression across population expansion. Panels: 1, MSC markers; 2, wound healing markers; 3, immune regulation markers; 4, ASC markers, 5, differentiation capacity markers. ASC; adipose-derived stromal/stem cells, CD; cluster of differentiation, Passage 1–8 (P1–8). The data are presented as means + standard deviation, n = 7–8, * indicates a statistically significant change $p < 0.05$.

Based on kinetic profiles, it was possible to classify the markers into three categories, where the spread of values converged during the culture onto a highly predictable value, remained constantly low irrespective of high or low expression levels, or was high due to individually markedly discordant expression patterns, as shown in Figure 3.

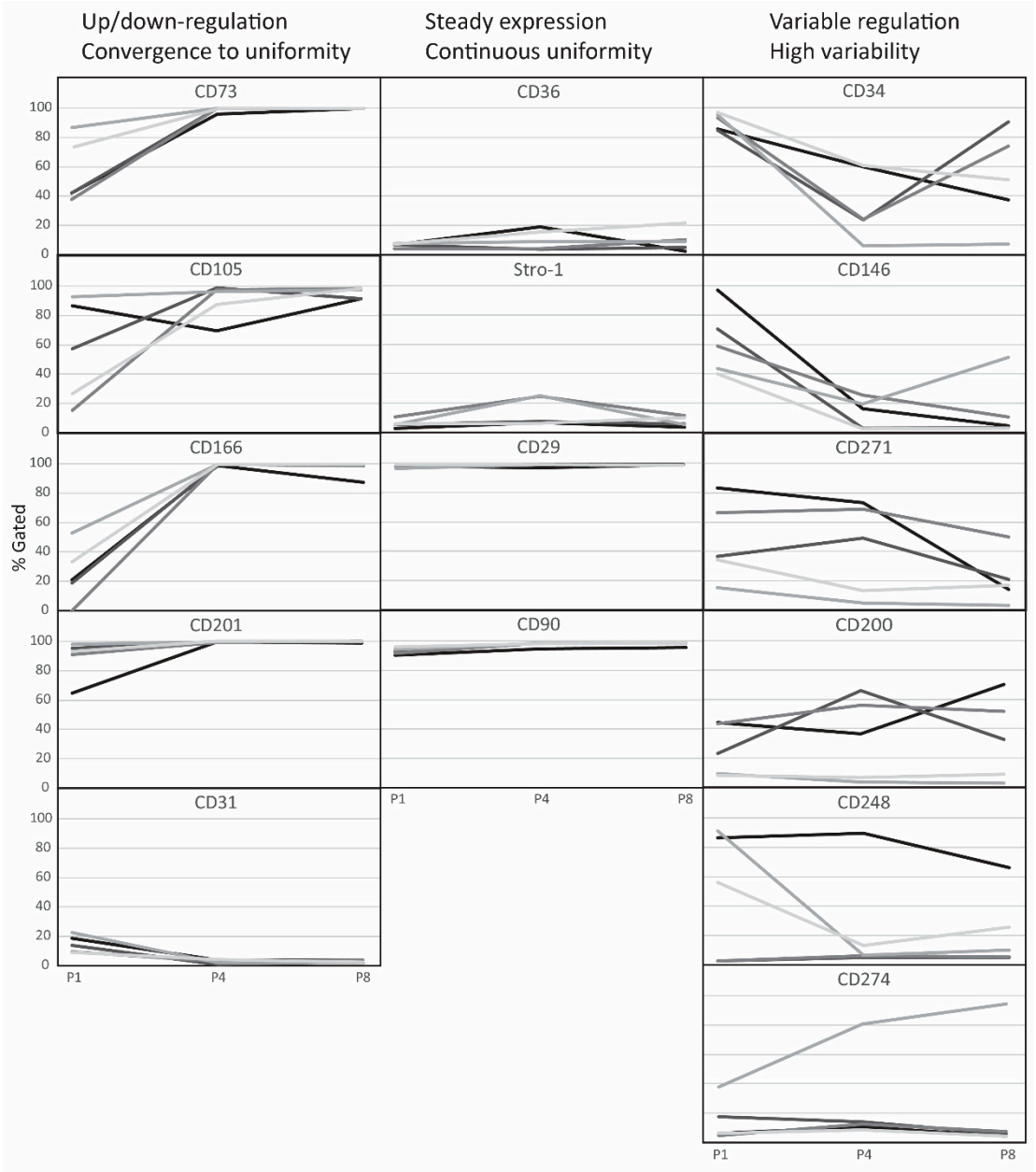

Figure 3. Kinetic profiles of single-marker expression across population expansion. Traces from 5 donors are shown at passages P1, P4, and P8. CD; cluster of differentiation, P; passage.

2.2. Evolution of Co-Expression Patterns

The prevalence of complex immunophenotypes within the functional panels and their temporal changes over eight passages are presented in Figure 4. Overall, only a limited number of variants out of all possible marker combinations was identified, and two distinct evolutionary patterns were discernible. In the majority of cases (Panels 1, 2, and 4), the spectrum of examined triple combinations was rather broad early in the culture (P1) but became rapidly reduced at the following passage or P4 at the latest. Interestingly, these changes are also coincident with the increase in the uniformity of cell cultures, as described in the previous section. The selected combinations then continued being stably expressed for the remainder of the culture. In the other pattern, there were few dominant immunophenotypical variants that remained present throughout the whole culture period. The quantitative relationships between early and late passages are presented in more detail in Figure S1. Furthermore, it should

be noted that the evolution of some particular phenotypes was clearly donor-dependent. Donor 1 exhibited particularly significant discrepancies, mostly in Panel 2, but also in Panels 4 and 5 (Figure S2).

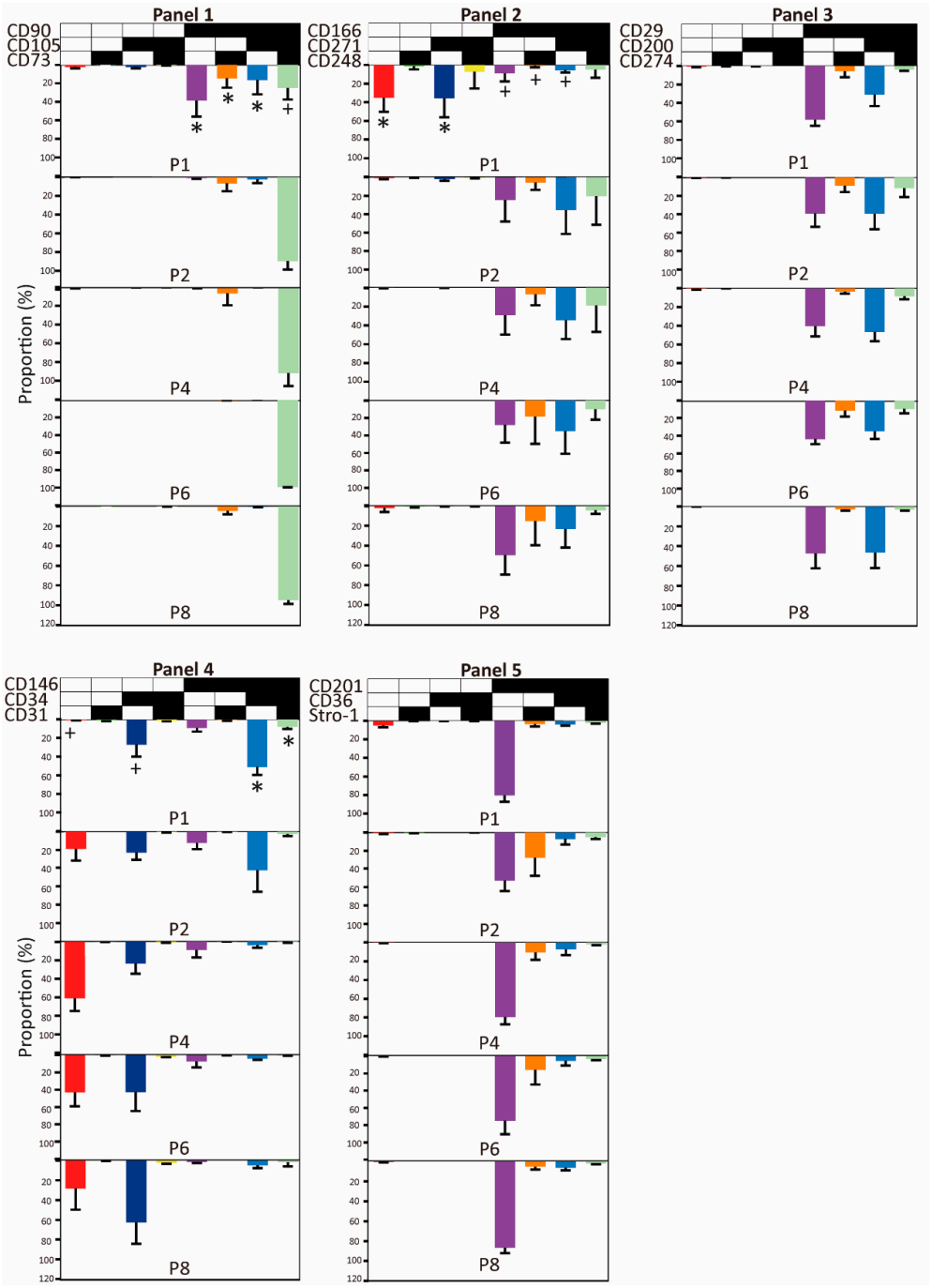

Figure 4. The prevalence of complex immunophenotypes within the functional panels and their temporal changes over eight passages. Panels: 1, mesenchymal stem cell (MSC) markers; 2, wound healing markers; 3, immune regulation markers; 4, Adipose-derived stromal/stem cell (ASC) markers, 5, differentiation capacity markers. A black field indicates that the marker was expressed; A white field indicates that the marker was not expressed. The data are presented as means + standard deviation, n = 7–8. *: population with the given combination of markers significantly decreases during culture. +: population with the given combination of markers significantly increases during culture. CD; cluster of differentiation.

In order to obtain a better understanding of the evolutionary processes in the cultures, we looked into what shifts in the marker expression occurred as a result of continued culturing (Figure 5). Regarding Panel 1, a convergence from single- or double-expressed markers to a triple co-expression took place. In Panel 2, the phenotypes switched through the acquisition of single CD166, and in Panel 4, a divergence occurred where the CD146+CD34+ phenotype shed only the CD146 or both the CD146 and CD34.

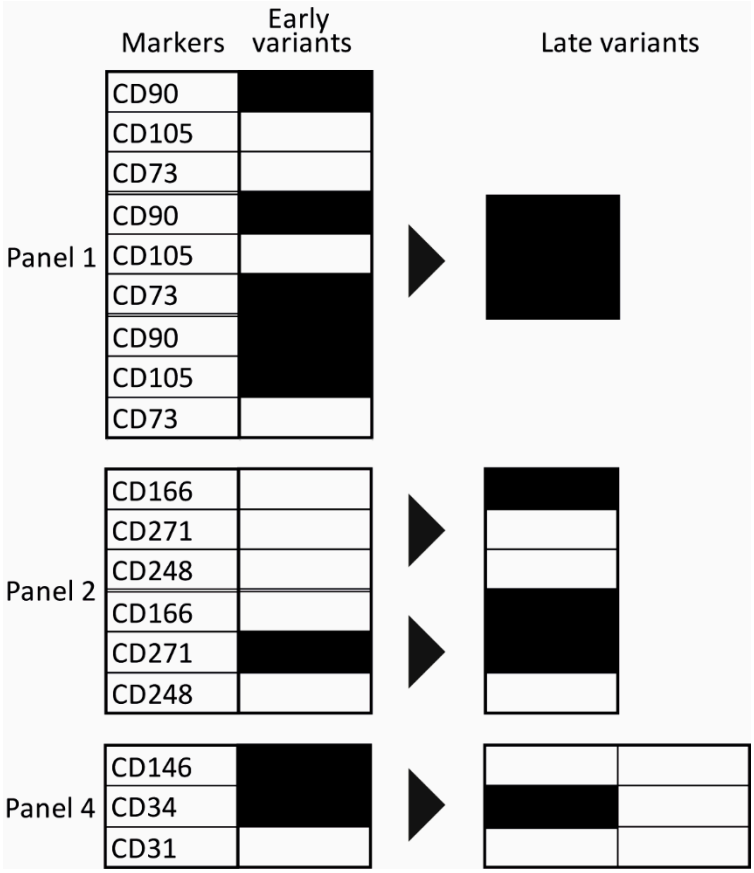

Figure 5. Evolution of predominant phenotypical variants. Panels: 1, mesenchymal stem cell (MSC) markers; 2, wound healing markers; 4, Adipose-derived stromal/stem cell (ASC) markers. A black field indicates that the marker was expressed, a white field indicates that the marker was not expressed. The black arrow reflects the evolution trend from the early stage to later culturing.

3. Discussion

ASCs hold great promise for emerging cell-based therapies and tissue engineering. Previous research has demonstrated that ASC cultures are actually a mixture of diverse phenotypes, presumably with different functionalities, and with a transcriptional pattern which evolves along with the expansion of the population [39,46]. Moreover, donor variation and fat tissue origin are additional contributing factors that have a major influence on the prevalence of particular immunophenotypes [18,36,47]. It can be speculated that these factors may be the source of variation between studies and the reason for suboptimal outcomes of some pre-clinical and clinical trials [36,48–52] and that it is plausible that by establishing a reliable association between some predictive biomarkers, such as surface membrane immunophenotype and clinical efficacy, ASC potential could be exploited to its fullest in the future. To date, the evolution of complex co-expressed immunophenotypic repertoires within ASC cultures has not been explored in a systematic fashion. Thus, as a first step, we have in the current study invoked 15 well-defined surface epitopes and followed their temporal changes in triple co-expression pattern using fat samples from five independent donors.

Not surprisingly, our investigation of single-marker expression corroborated well-established evidence regarding the uniform expression of hallmark antigens CD73, CD90, CD105, CD166, and CD29, and absence of CD31 in stages following P0 [17,18,46,53–56]. Nevertheless, some substantial discrepancies in previous data were uncovered with several markers as well. For instance, while the CD34 has initially been claimed not expressed [13] and some authors later were able to detect it in the early stages after primary isolation [46,57], our experiments revealed a robust expression between 30% and 90% (Figure 2). By the same token, in the light of previous reports indicating lack of expression of Stro-1 [20] which in retrospect may be attributed to antibody sources and detection methods [58], we could consistently identify this marker—albeit at a wide span of levels—ranging from around 3% to more than 50%, supporting the findings of Ning et al. and Zuk et al. [59,60]. This may be of biological importance due to Stro-1 being involved in clonogenicity, homing, and angiogenesis [7]. Less dramatic, though still considerable differences in expression levels were noticed for other surface markers, including CD36, CD146, CD200, CD201, and CD271 [18,34,61–63]. When using quantitative immunofluorescence techniques, such as multicolour flow cytometry, it is difficult to achieve absolute accuracy, unless highly prevalent and expressed epitopes are searched for. Additionally, results may vary depending on experimental set-up and instrumentation; proper cross-bleed compensation is also critical. Inconsistencies among data from independent laboratories, which can, for the most part, be attributed to donor- and/or tissue-source-related idiosyncrasies, can further be burdened by these experimental artefacts. It is therefore imperative that the subjects and procedures involved in tissue processing and marker analysis be adequately described and standardized as much as possible. Having previously been faced with the pitfalls of the multichromatic fluorescence cell sorting [12], it is our assumption that the discrepancies reported herewith are mostly attributable to the biological nature of our samples.

Despite the fact that our study enabled direct exploration of only triple marker combinations, based on the temporal patterns of individual markers as highlighted above, it is possible to infer that after the initial few passages, all cells came to express the common phenotype CD73+CD90+CD105+CD166+CD29+CD201+. The CD73+CD90+CD105+ triple positivity denotes stem/progenitor cells [13], and it is interesting that these cells became enriched by in vitro growth. Similarly, it is intriguing that a subset of these cells exhibiting the CD31−CD34+CD146− profile, previously found to identify a stem cell lineage [25,64,65], also grew proportionally to the culture period. In addition, possibly important ramifications may reveal that some antigens that have been ambiguously associated with stemness, including CD200, CD248, and CD271 [66,67], were reinforced during the culture, while all subsets featuring CD146, which has previously been recognized as a surrogate for stemness [40,68–71] were sequestered. Concerning interpersonal variability, the spread of the data roughly follows previously reported trends [49,72], except for two specific subsets, the CD166+CD271−CD248+ and CD166+CD271+CD248+, which were identified only in a single donor. It seems reasonable to assume that similar variations underlie, at least in part, the unique properties observed with some donors [36,52,73,74], but implications for providing a carrier with a selective advantage through a specific biological mechanism remain to be elucidated. In the light of a clinical advantage, researchers are beginning to look into the biological mechanism of specific co-expressed surface marker profiles [75–77]. It was found that CD34/CD90 double-positive cells was present after 30-days of expansion and that they may play a vital role in tissue reconstruction. Additionally, we have earlier found the subpopulation CD73+CD90+CD105+CD34-CD146+CD271− to have a positive effect on endothelial cells [12]. Consequently, it is worth continuing investigations of the biological effects of these interesting subsets to gain a more comprehensive understanding of the mechanism of action of ASCs.

Based on our data, it is obvious that even after a major homogenization of the immunophenotypical repertoire taking place at P1, stabilized discrete lineages remain within the culture population that can be discriminated, at least in our case, by the expression of CD34, CD200, CD248, and CD271. It appears worthwhile that the highly defined subpopulations within ASC cultures are to be studied using at least

a set of markers as outlined in this study, since such an investigation might reveal hitherto unknown relationships between the immunophenotypical profiles and functionality. This kind of information may be greatly beneficial for improving the efficacy of future ASC therapeutic applications.

4. Materials and Methods

4.1. ASC Isolation and Expansion

Adipose tissue samples used in this study were derived from five healthy donors who underwent cosmetic liposuction surgery at Aarhus University Hospital, Aarhus, Denmark or Aleris-Hamlet Private Hospital, Aalborg, Denmark. Written informed consent was obtained from each donor prior to donation, and our study was approved by the regional committee on biomedical research ethics on Northern Jutland (Project No. N-20160025, 17 April 2016). Tissue was collected according to Danish legislation on anonymized tissue (Komitélov §14), and the collection complied with the principles defined by the Declaration of Helsinki. ASCs were isolated as described previously in our laboratory [78]. In brief, after being washed four times with sterile phosphate-buffered saline (PBS; Gibco, Taastrup, Denmark), adipose tissue was digested with 0.6 U/mL collagenase NB 4 standard grade (Nordmark Biochemicals, Uetersen, Germany) in Hanks' Balanced Salt Solution (Gibco, Taastrup, Denmark) for 1 h at 37 °C under continuous agitation. The obtained dissociated tissue was filtered through a 100 µm filter (Millipore, Omaha, NE, USA) followed by low-speed centrifugation at 400× *g* for 10 min. After removing the supernatant, the cell pellet was resuspended in growth media that was alpha-Minimum Essential Medium with GlutaMAX supplemented with 10% fetal calf serum (FCS) and 1% antibiotics (all from Gibco, Taastrup, Denmark), filtered through a 60 µm filter (Millipore Omaha, NE, USA), and, finally, centrifuged at 400 g for 10 min.

The acquired cell pellet was resuspended in the growth medium, and cell yield was determined by the Nucleocounter NC-200 cell counter (Chemometec, Allerod, Denmark). Consequently, the resulting cells were seeded into T175 culture flasks (Greiner Bio-one, Frickenhausen, Germany), and these initial cultures were referred to as passage 0 (P0). At 70%–80% confluency, the cells were detached using TryPLE (Gibco, Taastrup, Denmark), and all the following cultures (P1–P8) were initiated at a density of 5000 cells/cm^2 [30]. During culture, the medium was changed every 2–3 days.

4.2. Multichromatic Flow Cytometry

Initially, ASCs from three donors were analyzed at P1, 2, 4, 6, and 8 in regard to 15 selected surface epitopes. To further examine the range of inter-donor variability, two additional donors were included in passages P1, 4, and 8. The 15 directly-labeled antibodies used to detect the surface epitopes were assorted in five panels of triple combinations based on functionality (Table 1) and used simultaneously with Fixable Viability Stain 570 (FVS570) (BD Biosciences, Lyngby, Denmark) to exclude the dead cells from analysis. For technical details about antibodies, see Table A1. For staining, cell suspensions were first filtered through a cell strainer (70 µm; BD Falcon; BD Bioscience, Erembodegem, Belgium) and subsequently dispensed at 2×10^5 cells per reaction tube. Cells were initially incubated with the viability reagent for 15 min at room temperature, after which a mixture of antibodies optimally diluted in PBS supplemented with 2% FCS and 0.1% sodium azide (Merck Schuchardt, Hohenbrunn, Germany) was added. In Panel 5, where two or more BD Horizon Brilliant dyes were used, BD Horizon Brilliant Stain Buffer (BD Bioscience, Erembodegem, Belgium) was used as a diluent. After staining for 30 min at 4 °C in the dark, the samples were washed twice with 50% Accumax (Sigma-Aldrich, Copenhagen, Denmark) in PBS to prevent cell aggregation. For each panel at each passage, two or three independent staining experiments were conducted.

For surface epitope analysis, a CytoFLEX (Beckman coulter, Copenhagen, Denmark) flow cytometer was employed. Prior to analyzing the samples, compensation values were established with the aid of the BD CompBeads Plus Set Anti-mouse Ig, κ and Anti-rat Ig, κ (BD Biosciences, Erembodegem, Belgium) and invoking a compensation matrix based on the dot-plots delineating the combination of

channels used in the particular experiment. The data were visualized and analyzed in the Kaluza 2.1 software package (Beckman Coulter, Indianapolis, IN, USA). To validate data analysis, four gates were adopted: one to remove debris (forward scatter area vs. side scatter area); one to ensure cell flow and flow cytometer stability (forward scatter area vs. time); one to discriminate doublets (forward scatter area versus forward scatter height); and one to eliminate dead cell (viability dye intensity histogram). Fluorescence minus one (FMO) controls were used to define the cutoff limit for background values, which was generically set at 97.5th percentile. The gating strategy can be seen in Figure A1.

4.3. Statistical Analysis

The data entailing 2–3 replicates for each passage derived from each of the three donors were presented as mean + standard deviation (SD). The General Linear Model (GLM) procedure with repeated measures followed by post-hoc tests of the IBM SPSS Statistics v.26 software package (IBM, Armonk, NY, USA) was utilized to assess the differences between the passages and donors. The level of significance was set at 0.05.

Supplementary Materials: Supplementary Materials can be found at http://www.mdpi.com/1422-0067/21/4/1408/s1.

Author Contributions: Conceptualization, S.P., T.F., and V.Z.; methodology, Q.P. and H.A.; investigation, Q.P.; resources, T.F. and V.Z.; data curation, Q.P. and V.Z.; writing—original draft preparation, Q.P. and V.Z.; writing—review and editing, H.A., S.P., and T.F.; visualization, Q.P. and V.Z.; supervision, V.Z.; project administration, V.Z.; funding acquisition, V.Z. All authors have read and agreed to the published version of the manuscript.

Funding: This research received no external funding. The first author was supported by the China Scholarship Council.

Acknowledgments: The authors would like to thank Frederik Mølgaard Nielsen for the technical aid with the flow cytometry.

Conflicts of Interest: The authors declare no conflict of interest. The funders had no role in the design of the study; in the collection, analyses, or interpretation of data; in the writing of the manuscript, or in the decision to publish the results.

Abbreviations

ASC	Adipose-derived stromal/stem cells
BP	Band pass
CD	Cluster of differentiation
FCS	Fetal calf serum
FMO	Fluorescence minus one
FSC-A	Forward scatter area
FSC-H	Forward scatter hight
FVS570	Fixable viability stain 570
GLM	General linear model
MSC	Mesenchymal stem cells
P	Passage
SD	Standard deviation
SSC-A	Side scatter area
SVF	Stromal vascular fraction

Appendix A

Table A1. Technical details on antibodies and reagents used for flow cytometry.

Fluorophore	Antigen	Host	Company	Catalog Number
BV421	CD201	rat	BD Biosciences	743552
BV510	CD105	mouse	BD Biosciences	563264
BV605	CD166	mouse	BD Biosciences	742373
APC-R700	CD274	mouse	BD Biosciences	565188
APC-Cy7	CD31	mouse	BD Biosciences	563653
FITC	CD73	mouse	BD Biosciences	561254
BV605	CD36	mouse	BD Biosciences	563518
BV650	CD29	mouse	BD Biosciences	743785
PE-Cy 7	CD200	mouse	BD Biosciences	562125
PE-Cy7	CD271	mouse	BD Biosciences	562122
Alexa Fluor 647	CD248	mouse	BD Biosciences	564994
Alexa Fluor 647	Stro-1	mouse	R & D system	FAB1038R
Percp-Cy5.5	CD90	mouse	BD Biosciences	561557
PE-CF594	CD146	mouse	BD Biosciences	564327
PE-Cy7	CD34	mouse	BD Biosciences	560710
Product Name			**Company**	**Catalog Number**
BD Horizon™ Brilliant Stain Buffer			BD Biosciences	563794
Viability dye, FVS570			BD Biosciences	564995
CompBeads Plus Set Anti-mouse Ig, κ			BD Biosciences	560497
CompBeads Plus Set Anti-rat Ig, κ			BD Biosciences	560499

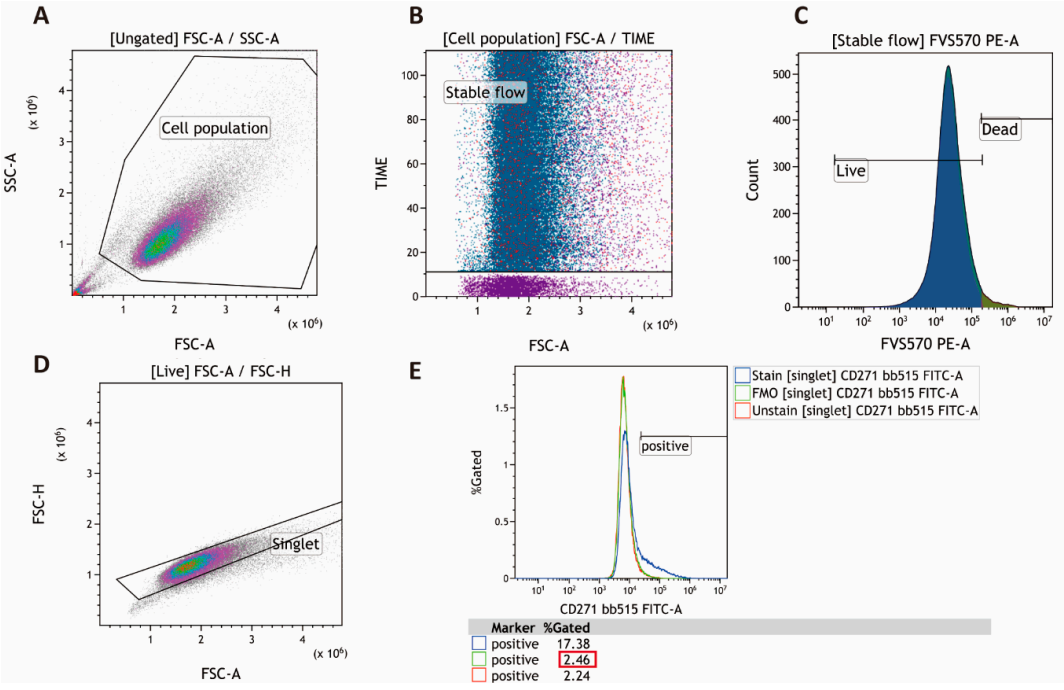

Figure A1. Gating strategy for flow cytometry. (**A**) Noise was removed to collect the cell population using forward scatter area (FSC-A) versus side scatter area (SSC-A). (**B**) To ensure a stable flow during data aquisition, the FSC-A versus time plot was controlled. (**C**) To exclude dead cells, viability dye (FVS570) was used. (**D**) The doublets were discriminated via FSC-A versus forward scatter height (FSC-H). (**E**) Representative of the overlay histogram of the unstained, fluorescence minus one (FMO) and stained group. Red box: the threshold was set at the 2.5% of FMO.

References

1. Bajek, A.; Gurtowska, N.; Olkowska, J.; Kazmierski, L.; Maj, M.; Drewa, T. Adipose-Derived Stem Cells as a Tool in Cell-Based Therapies. *Arch. Immunol. Ther. Exp. (Warsz.)* **2016**, *64*, 443–454. [CrossRef] [PubMed]
2. Strioga, M.; Viswanathan, S.; Darinskas, A.; Slaby, O.; Michalek, J. Same or not the same? Comparison of adipose tissue-derived versus bone marrow-derived mesenchymal stem and stromal cells. *Stem Cells Dev.* **2012**, *21*, 2724–2752. [CrossRef] [PubMed]
3. Berry, D.C.; Jiang, Y.; Graff, J.M. Emerging Roles of Adipose Progenitor Cells in Tissue Development, Homeostasis, Expansion and Thermogenesis. *Trends Endocrinol. Metab.* **2016**, *27*, 574–585. [CrossRef] [PubMed]
4. Badimon, L.; Cubedo, J. Adipose tissue depots and inflammation: Effects on plasticity and residentmesenchymal stem cell function. *Cardiovasc. Res.* **2017**, *113*, 1064–1073. [CrossRef]
5. Cao, F.; Liu, T.; Xu, Y.; Xu, D.; Feng, S. Culture and properties of adipose-derived mesenchymal stem cells: Characteristics in vitro and immunosuppression in vivo. *Int. J. Clin. Exp. Pathol.* **2015**, *8*, 7694–7709.
6. Larsen, L.; Tchanque-Fossuo, C.N.; Gorouhi, F.; Boudreault, D.; Nguyen, C.; Fuentes, J.J.; Crawford, R.W.; Dahle, S.E.; Whetzel, T.; Rivkah Isseroff, R. Combination therapy of autologous adipose mesenchymal stem cell-enriched, high-density lipoaspirate and topical timolol for healing chronic wounds. *J. Tissue Eng. Regen. Med.* **2018**, *12*, 186–190. [CrossRef]
7. Moon, K.C.; Suh, H.S.; Kim, K.B.; Han, S.K.; Young, K.W.; Lee, J.W.; Kim, M.H. Potential of allogeneic adipose-derived stem cell–hydrogel complex for treating diabetic foot ulcers. *Diabetes* **2019**, *68*, 837–846. [CrossRef]
8. Tang, Y.; Pan, Z.Y.; Zou, Y.; He, Y.; Yang, P.Y.; Tang, Q.Q.; Yin, F. A comparative assessment of adipose-derived stem cells from subcutaneous and visceral fat as a potential cell source for knee osteoarthritis treatment. *J. Cell. Mol. Med.* **2017**, *21*, 2153–2162. [CrossRef]
9. Badimon, L.; Oñate, B.; Vilahur, G. Adipose-derived Mesenchymal Stem Cells and Their Reparative Potential in Ischemic Heart Disease. *Rev. Española Cardiol. Engl. Ed.* **2015**, *68*, 599–611. [CrossRef]
10. Lin, H.P.; Chan, T.M.; Fu, R.H.; Chuu, C.P.; Chiu, S.C.; Tseng, Y.H.; Liu, S.P.; Lai, K.C.; Shih, M.C.; Lin, Z.S.; et al. Applicability of adipose-derived stem cells in type 1 diabetes mellitus. *Cell Transplant.* **2015**, *24*, 521–532. [CrossRef]
11. Dominici, M.; Paolucci, P.; Conte, P.; Horwitz, E.M. Heterogeneity of Multipotent Mesenchymal Stromal Cells: From Stromal Cells to Stem Cells and Vice Versa. *Transplantation* **2009**, *87*, S36–S42. [CrossRef] [PubMed]
12. Nielsen, F.M.; Riis, S.E.; Andersen, J.I.; Lesage, R.; Fink, T.; Pennisi, C.P.; Zachar, V. Discrete adipose-derived stem cell subpopulations may display differential functionality after in vitro expansion despite convergence to a common phenotype distribution. *Stem Cell Res. Ther.* **2016**, *7*, 177. [CrossRef] [PubMed]
13. Dominici, M.; Le Blanc, K.; Mueller, I.; Slaper-Cortenbach, I.; Marini, F.; Krause, D.; Deans, R.; Keating, A.; Prockop, D.; Horwitz, E. Minimal criteria for defining multipotent mesenchymal stromal cells. The International Society for Cellular Therapy position statement. *Cytotherapy* **2006**, *8*, 315–317. [CrossRef] [PubMed]
14. Maslova, O.O. Current view of mesenchymal stem cells biology (Brief review). *Biopolym. Cell* **2012**, *28*, 190–198. [CrossRef]
15. Levi, B.; Wan, D.C.; Glotzbach, J.P.; Hyun, J.; Januszyk, M.; Montoro, D.; Sorkin, M.; James, A.W.; Nelson, E.R.; Li, S.; et al. CD105 protein depletion enhances human adipose-derived stromal cell osteogenesis through reduction of transforming growth factor β1 (TGF-β1) signaling. *J. Biol. Chem.* **2011**, *286*, 39497–39509. [CrossRef]
16. Chung, M.T.; Liu, C.; Hyun, J.S.; Lo, D.D.; Montoro, D.T.; Hasegawa, M.; Li, S.; Sorkin, M.; Rennert, R.; Keeney, M.; et al. CD90 (Thy-1)-Positive Selection Enhances Osteogenic Capacity of Human Adipose-Derived Stromal Cells. *Tissue Eng. Part A* **2013**, *19*, 989–997. [CrossRef]
17. Yang, S.; Pilgaard, L.; Chase, L.G.; Boucher, S.; Vemuri, M.C.; Fink, T.; Zachar, V. Defined xenogeneic-free and hypoxic environment provides superior conditions for long-term expansion of human adipose-derived stem cells. *Tissue Eng. Part C Methods* **2012**, *18*, 593–602. [CrossRef]
18. Baer, P.C.; Kuçi, S.; Krause, M.; Kuçi, Z.; Zielen, S.; Geiger, H.; Bader, P.; Schubert, R. Comprehensive Phenotypic Characterization of Human Adipose-Derived Stromal/Stem Cells and Their Subsets by a High Throughput Technology. *Stem Cells Dev.* **2012**, *22*, 330–339. [CrossRef]

19. Mildmay-White, A.; Khan, W. Cell Surface Markers on Adipose-Derived Stem Cells: A Systematic Review. *Curr. Stem Cell Res. Ther.* **2017**, *12*, 484–492. [CrossRef]
20. Gronthos, S.; Franklin, D.M.; Leddy, H.A.; Robey, P.G.; Storms, R.W.; Gimble, J.M. Surface protein characterization of human adipose tissue-derived stromal cells. *J. Cell. Physiol.* **2001**, *189*, 54–63. [CrossRef]
21. Astori, G.; Vignati, F.; Bardelli, S.; Tubio, M.; Gola, M.; Albertini, V.; Bambi, F.; Scali, G.; Castelli, D.; Rasini, V.; et al. "In vitro" and multicolor phenotypic characterization of cell subpopulations identified in fresh human adipose tissue stromal vascular fraction and in the derived mesenchymal stem cells. *J. Transl. Med.* **2007**, *5*, 55. [CrossRef] [PubMed]
22. Riis, S.; Zachar, V.; Boucher, S.; Vemuri, M.C.; Pennisi, C.P.; Fink, T. Critical steps in the isolation and expansion of adipose-derived stem cells for translational therapy. *Expert Rev. Mol. Med.* **2015**, *17*, e11. [CrossRef] [PubMed]
23. Gao, H.; Volat, F.; Sandhow, L.; Galitzky, J.; Nguyen, T.; Esteve, D.; Åström, G.; Mejhert, N.; Ledoux, S.; Thalamas, C.; et al. CD36 Is a Marker of Human Adipocyte Progenitors with Pronounced Adipogenic and Triglyceride Accumulation Potential. *Stem Cells* **2017**, *35*, 1799–1814. [CrossRef] [PubMed]
24. Brett, E.; Zielins, E.R.; Chin, M.; Januszyk, M.; Blackshear, C.P.; Findlay, M.; Momeni, A.; Gurtner, G.C.; Longaker, M.T.; Wan, D.C. Isolation of CD248-expressing stromal vascular fraction for targeted improvement of wound healing. *Wound Repair Regen.* **2017**, *25*, 414–422. [CrossRef] [PubMed]
25. Beckenkamp, L.R.; Souza, L.E.B.; Melo, F.U.F.; Thomé, C.H.; Magalhães, D.A.R.; Palma, P.V.B.; Covas, D.T. Comparative characterization of CD271+ and CD271− subpopulations of CD34+ human adipose-derived stromal cells. *J. Cell. Biochem.* **2018**, *119*, 3873–3884. [CrossRef]
26. Mihaila, S.M.; Frias, A.M.; Pirraco, R.P.; Rada, T.; Reis, R.L.; Gomes, M.E.; Marques, A.P. Human adipose tissue-derived SSEA-4 subpopulation multi-differentiation potential towards the endothelial and osteogenic lineages. *Tissue Eng. Part A* **2013**, *19*, 235–246. [CrossRef]
27. Rada, T.; Santos, T.C.; Marques, A.P.; Correlo, V.M.; Frias, A.M.; Castro, A.G.; Neves, N.M.; Gomes, M.E.; Reis, R.L. Osteogenic differentiation of two distinct subpopulations of human adipose-derived stem cells: An in vitro and in vivo study. *J. Tissue Eng. Regen. Med.* **2012**, *6*, 1–11. [CrossRef]
28. Li, H.; Zimmerlin, L.; Marra, K.G.; Donnenberg, V.S.; Donnenberg, A.D.; Rubin, J.P. Adipogenic potential of adipose stem cell subpopulations. *Plast. Reconstr. Surg.* **2011**, *128*, 663–672. [CrossRef]
29. Najar, M.; Raicevic, G.; Jebbawi, F.; De Bruyn, C.; Meuleman, N.; Bron, D.; Toungouz, M.; Lagneaux, L. Characterization and functionality of the CD200-CD200R system during mesenchymal stromal cell interactions with T-lymphocytes. *Immunol. Lett.* **2012**, *146*, 50–56. [CrossRef]
30. Psaltis, P.J.; Paton, S.; See, F.; Arthur, A.; Martin, S.; Itescu, S.; Worthley, S.G.; Gronthos, S.; Zannettino, A.C.W. Enrichment for STRO-1 expression enhances the cardiovascular paracrine activity of human bone marrow-derived mesenchymal cell populations. *J. Cell. Physiol.* **2010**, *223*, 530–540. [CrossRef]
31. Bruder, S.P.; Ricalton, N.S.; Boynton, R.E.; Connolly, T.J.; Jaiswal, N.; Zaia, J.; Barry, F.P. Mesenchymal stem cell surface antigen SB-10 corresponds to activated leukocyte cell adhesion molecule and is involved in osteogenic differentiation. *J. Bone Miner. Res.* **1998**, *13*, 655–663. [CrossRef] [PubMed]
32. Sanders, A.J.; Jiang, D.G.; Jiang, W.G.; Harding, K.G.; Patel, G.K. Activated leukocyte cell adhesion molecule impacts on clinical wound healing and inhibits HaCaT migration. *Int. Wound J.* **2011**, *8*, 500–507. [CrossRef]
33. Luz-Crawford, P.; Noël, D.; Fernandez, X.; Khoury, M.; Figueroa, F.; Carrión, F.; Jorgensen, C.; Djouad, F. Mesenchymal Stem Cells Repress Th17 Molecular Program through the PD-1 Pathway. *PLoS ONE* **2012**, *7*. [CrossRef]
34. Camilleri, E.T.; Gustafson, M.P.; Dudakovic, A.; Riester, S.M.; Garces, C.G.; Paradise, C.R.; Takai, H.; Karperien, M.; Cool, S.; Sampen, H.J.I.; et al. Identification and validation of multiple cell surface markers of clinical-grade adipose-derived mesenchymal stromal cells as novel release criteria for good manufacturing practice-compliant production. *Stem Cell Res. Ther.* **2016**, *7*. [CrossRef] [PubMed]
35. Miyata, Y.; Otsuki, M.; Kita, S.; Shimomura, I. Identification of Mouse Mesenteric and Subcutaneous in vitro Adipogenic Cells. *Sci. Rep.* **2016**, *6*, 21041. [CrossRef] [PubMed]
36. Ong, W.K.; Tan, C.S.; Chan, K.L.; Goesantoso, G.G.; Chan, X.H.D.; Chan, E.; Yin, J.; Yeo, C.R.; Khoo, C.M.; So, J.B.Y.; et al. Identification of Specific Cell-Surface Markers of Adipose-Derived Stem Cells from Subcutaneous and Visceral Fat Depots. *Stem Cell Rep.* **2014**, *2*, 171–179. [CrossRef] [PubMed]

37. Durandt, C.; van Vollenstee, F.A.; Dessels, C.; Kallmeyer, K.; de Villiers, D.; Murdoch, C.; Potgieter, M.; Pepper, M.S. Novel flow cytometric approach for the detection of adipocyte subpopulations during adipogenesis. *J. Lipid Res.* **2016**, *57*, 729–742. [CrossRef]
38. Bourin, P.; Bunnell, B.A.; Casteilla, L.; Dominici, M.; Katz, A.J.; March, K.L.; Redl, H.; Rubin, J.P.; Yoshimura, K.; Gimble, J.M. Stromal cells from the adipose tissue-derived stromal vascular fraction and culture expanded adipose tissue-derived stromal/stem cells: A joint statement of the International Federation for Adipose Therapeutics and Science (IFATS) and the International So. *Cytotherapy* **2013**, *15*, 641–648. [CrossRef]
39. Baer, P.C. Adipose-derived mesenchymal stromal/stem cells: An update on their phenotype in vivo and in vitro. *World J. Stem Cells* **2014**, *6*, 256–265. [CrossRef]
40. Lee, N.E.; Kim, S.J.; Yang, S.J.; Joo, S.Y.; Park, H.; Lee, K.W.; Yang, H.M.; Park, J.B. Comparative characterization of mesenchymal stromal cells from multiple abdominal adipose tissues and enrichment of angiogenic ability via CD146 molecule. *Cytotherapy* **2017**, *19*, 170–180. [CrossRef]
41. Davies, O.G.; Cooper, P.R.; Shelton, R.M.; Smith, A.J.; Scheven, B.A. Isolation of adipose and bone marrow mesenchymal stem cells using CD29 and CD90 modifies their capacity for osteogenic and adipogenic differentiation. *J. Tissue Eng.* **2015**, *6*. [CrossRef] [PubMed]
42. Rada, T.; Reis, R.L.; Gomes, M.E. Distinct stem cells subpopulations isolated from human adipose tissue exhibit different chondrogenic and osteogenic differentiation potential. *Stem Cell Rev. Rep.* **2011**, *7*, 64–76. [CrossRef] [PubMed]
43. Ip, J.E.; Wu, Y.; Huang, J.; Zhang, L.; Pratt, R.E.; Dzau, V.J. Mesenchymal stem cells use integrin β1 not CXC chemokine receptor 4 for myocardial migration and engraftment. *Mol. Biol. Cell* **2007**, *18*, 2873–2882. [CrossRef]
44. Calabrese, G.; Giuffrida, R.; Lo Furno, D.; Parrinello, N.L.; Forte, S.; Gulino, R.; Colarossi, C.; Schinocca, L.R.; Giuffrida, R.; Cardile, V.; et al. Potential effect of CD271 on human mesenchymal stromal cell proliferation and differentiation. *Int. J. Mol. Sci.* **2015**, *16*, 15609–15624. [CrossRef] [PubMed]
45. Latifi-Pupovci, H.; Kuçi, Z.; Wehner, S.; Bönig, H.; Lieberz, R.; Klingebiel, T.; Bader, P.; Kuçi, S. In vitro migration and proliferation ("wound healing") potential of mesenchymal stromal cells generated from human CD271(+) bone marrow mononuclear cells. *J. Transl. Med.* **2015**, *13*, 315. [CrossRef] [PubMed]
46. Mitchell, J.B.; McIntosh, K.; Zvonic, S.; Garrett, S.; Floyd, Z.E.; Kloster, A.; Di Halvorsen, Y.; Storms, R.W.; Goh, B.; Kilroy, G.; et al. Immunophenotype of Human Adipose-Derived Cells: Temporal Changes in Stromal-Associated and Stem Cell-Associated Markers. *Stem Cells* **2006**, *24*, 376–385. [CrossRef] [PubMed]
47. Prieto González, E.A. Heterogeneity in Adipose Stem Cells. In *Advances in Experimental Medicine and Biology*; Springer: New York, NY, USA, 2019; Volume 1123, pp. 119–150.
48. Yang, H.J.; Kim, K.J.; Kim, M.K.; Lee, S.J.; Ryu, Y.H.; Seo, B.F.; Oh, D.Y.; Ahn, S.T.; Lee, H.Y.; Rhie, J.W. The stem cell potential and multipotency of human adipose tissue-derived stem cells vary by cell donor and are different from those of other types of stem cells. *Cells Tissues Organs* **2014**, *199*, 373–383. [CrossRef]
49. Reumann, M.K.; Linnemann, C.; Aspera-Werz, R.H.; Arnold, S.; Held, M.; Seeliger, C.; Nussler, A.K.; Ehnert, S. Donor site location is critical for proliferation, stem cell capacity, and osteogenic differentiation of adipose mesenchymal stem/stromal cells: Implications for bone tissue engineering. *Int. J. Mol. Sci.* **2018**, *19*, 1868. [CrossRef]
50. Chaker, D.; Mouawad, C.; Azar, A.; Quilliot, D.; Achkar, I.; Fajloun, Z.; Makdissy, N. Inhibition of the RhoGTPase Cdc42 by ML141 enhances hepatocyte differentiation from human adipose-derived mesenchymal stem cells via the Wnt5a/PI3K/miR-122 pathway: Impact of the age of the donor. *Stem Cell Res. Ther.* **2018**, *9*. [CrossRef]
51. Liu, M.; Lei, H.; Dong, P.; Fu, X.; Yang, Z.; Yang, Y.; Ma, J.; Liu, X.; Cao, Y.; Xiao, R. Adipose-Derived Mesenchymal Stem Cells from the Elderly Exhibit Decreased Migration and Differentiation Abilities with Senescent Properties. *Cell Transplant.* **2017**, *26*, 1505–1519. [CrossRef]
52. Guneta, V.; Tan, N.S.; Sugii, S.; Lim, T.C.; Wong, T.C.M.; Choong, C. Comparative study of adipose-derived stem cells from abdomen and breast. *Ann. Plast. Surg.* **2016**, *76*, 569–575. [CrossRef] [PubMed]
53. Donnenberg, A.D.; Meyer, E.M.; Rubin, J.P.; Donnenberg, V.S. The cell-surface proteome of cultured adipose stromal cells. *Cytom. Part A* **2015**, *87*. [CrossRef] [PubMed]
54. Walmsley, G.G.; Atashroo, D.A.; Maan, Z.N.; Hu, M.S.; Zielins, E.R.; Tsai, J.M.; Duscher, D.; Paik, K.; Tevlin, R.; Marecic, O.; et al. High-Throughput Screening of Surface Marker Expression on Undifferentiated and Differentiated Human Adipose-Derived Stromal Cells. *Tissue Eng. Part A* **2015**. [CrossRef] [PubMed]

55. Zuk, P. *Regenerative Medicine and Tissue Engineering*; Andrades, J.A., Ed.; InTech: London, UK, 2013; ISBN 978-953-51-1108-5.
56. Mafi, P. Adult Mesenchymal Stem Cells and Cell Surface Characterization-A Systematic Review of the Literature. *Open Orthop. J.* **2011**, *5*, 253–260. [CrossRef]
57. Yoshimura, K.; Shigeura, T.; Matsumoto, D.; Sato, T.; Takaki, Y.; Aiba-Kojima, E.; Sato, K.; Inoue, K.; Nagase, T.; Koshima, I.; et al. Characterization of freshly isolated and cultured cells derived from the fatty and fluid portions of liposuction aspirates. *J. Cell. Physiol.* **2006**, *208*, 64–76. [CrossRef]
58. Gimble, J.M.; Katz, A.J.; Bunnell, B.A. Adipose-derived stem cells for regenerative medicine. *Circ. Res.* **2007**, *100*, 1249–1260. [CrossRef]
59. Ning, H.; Lin, G.; Lue, T.F.; Lin, C.-S. Mesenchymal Stem Cell Marker Stro-1 is a 75kd Endothelial Antigen. *Biochem. Biophys. Res. Commun.* **2011**, *413*. [CrossRef]
60. Zuk, P.A.; Zhu, M.; Ashjian, P.; De Ugarte, D.A.; Huang, J.I.; Mizuno, H.; Alfonso, Z.C.; Fraser, J.K.; Benhaim, P.; Hedrick, M.H. Human adipose tissue is a source of multipotent stem cells. *Mol. Biol. Cell* **2002**, *13*, 4279–4295. [CrossRef]
61. Riis, S.; Nielsen, F.M.; Pennisi, C.P.; Zachar, V.; Fink, T. Comparative Analysis of Media and Supplements on Initiation and Expansion of Adipose-Derived Stem Cells. *Stem Cells Transl. Med.* **2016**, *5*, 314–324. [CrossRef]
62. Nepali, S.; Park, M.; Lew, H.; Kim, O. Comparative Analysis of Human Adipose-Derived Mesenchymal Stem Cells from Orbital and Abdominal Fat. *Stem Cells Int.* **2018**, *2018*. [CrossRef]
63. Dizaji Asl, K.; Shafaei, H.; Soleimani Rad, J.; Ollah Nozad, H. Comparison of Characteristics of Human Amniotic Membrane and Human Adipose Tissue Derived Mesenchymal Stem Cells. *World J. Plast. Surg.* **2017**, *6*, 33–39. [PubMed]
64. Zimmerlin, L.; Donnenberg, V.S.; Rubin, J.P.; Donnenberg, A.D. Mesenchymal markers on human adipose stem/progenitor cells. *Cytom. Part A* **2013**, *83A*, 134–140. [CrossRef] [PubMed]
65. Varma, M.J.O.; Breuls, R.G.M.; Schouten, T.E.; Jurgens, W.J.F.M.; Bontkes, H.J.; Schuurhuis, G.J.; Ham, S.M.V.; Milligen, F.J.V. Phenotypical and Functional Characterization of Freshly Isolated Adipose Tissue-Derived Stem Cells. *Stem Cells Dev.* **2007**, *16*, 91–104. [CrossRef] [PubMed]
66. Schachtele, S.; Clouser, C.; Aho, J. Markers and Methods to Verify Mesenchymal Stem Cell Identity, Potency, and Quality. Available online: https://www.rndsystems.com/cn/resources/articles/markers-and-methods-verify-mesenchymal-stem-cell-identity-potency-and-quality (accessed on 29 January 2020).
67. Lv, F.-J.; Tuan, R.S.; Cheung, K.M.C.; Leung, V.Y.L. Concise Review: The Surface Markers and Identity of Human Mesenchymal Stem Cells. *Stem Cells* **2014**, *32*, 1408–1419. [CrossRef]
68. Hörl, S.; Ejaz, A.; Ernst, S.; Mattesich, M.; Kaiser, A.; Jenewein, B.; Zwierzina, M.E.; Hammerle, S.; Miggitsch, C.; Mitterberger-Vogt, M.C.; et al. CD146 (MCAM) in human cs-DLK1−/cs-CD34+ adipose stromal/progenitor cells. *Stem Cell Res.* **2017**, *22*, 1–12. [CrossRef]
69. Crisan, M.; Yap, S.; Casteilla, L.; Chen, C.-W.; Corselli, M.; Park, T.S.; Andriolo, G.; Sun, B.; Zheng, B.; Zhang, L.; et al. A perivascular origin for mesenchymal stem cells in multiple human organs. *Cell Stem Cell* **2008**, *3*, 301–313. [CrossRef]
70. Li, X.; Guo, W.; Zha, K.; Jing, X.; Wang, M.; Zhang, Y.; Hao, C.; Gao, S.; Chen, M.; Yuan, Z.; et al. Enrichment of CD146+ adipose-derived stem cells in combination with articular cartilage extracellular matrix scaffold promotes cartilage regeneration. *Theranostics* **2019**, *9*, 5105–5121. [CrossRef]
71. Su, X.; Zuo, W.; Wu, Z.; Chen, J.; Wu, N.; Ma, P.; Xia, Z.; Jiang, C.; Ye, Z.; Liu, S.; et al. CD146 as a new marker for an increased chondroprogenitor cell sub-population in the later stages of osteoarthritis. *J. Orthop. Res.* **2015**, *33*, 84–91. [CrossRef]
72. Patel, R.S.; Carter, G.; El Bassit, G.; Patel, A.A.; Cooper, D.R.; Murr, M.; Patel, N.A. Adipose-derived stem cells from lean and obese humans show depot specific differences in their stem cell markers, exosome contents and senescence: Role of protein kinase C delta (PKCδ) in adipose stem cell niche. *Stem Cell Investig.* **2016**, *2016*. [CrossRef]
73. Nugraha Setyawan, E.M.; Oh, H.J.; Kim, M.J.; Kim, G.A.; Lee, S.H.; Choi, Y.B.; Ra, K.; Lee, B.C. Despite the donor's age, human adipose-derived stem cells enhance the maturation and development rates of porcine oocytes in a co-culture system. *Theriogenology* **2018**, *115*, 57–64. [CrossRef] [PubMed]
74. Kim, M.; Erickson, I.E.; Huang, A.H.; Garrity, S.T.; Mauck, R.L.; Steinberg, D.R. Donor Variation and Optimization of Human Mesenchymal Stem Cell Chondrogenesis in Hyaluronic Acid. *Tissue Eng. Part A* **2018**, *24*, 1693–1703. [CrossRef] [PubMed]

75. De Francesco, F.; Tirino, V.; Desiderio, V.; Ferraro, G.; D'andrea, F.; Giuliano, M.; Libondi, G.; Pirozzi, G.; De Rosa, A.; Papaccio, G. Human CD34 +/CD90 + ASCs Are Capable of Growing as Sphere Clusters, Producing High Levels of VEGF and Forming Capillaries. *PLoS ONE* **2009**, *4*. [CrossRef] [PubMed]
76. Ferraro, G.A.; De Francesco, F.; Nicoletti, G.; Paino, F.; Desiderio, V.; Tirino, V.; D'Andrea, F. Human adipose CD34+CD90+ stem cells and collagen scaffold constructs grafted in vivo fabricate loose connective and adipose tissues. *J. Cell. Biochem.* **2013**, *114*, 1039–1049. [CrossRef] [PubMed]
77. D'Andrea, F.; De Francesco, F.; Ferraro, G.A.; Desiderio, V.; Tirino, V.; De Rosa, A.; Papaccio, G. Large-scale production of human adipose tissue from stem cells: A new tool for regenerative medicine and tissue banking. *Tissue Eng. Part C Methods* **2008**, *14*, 233–242. [CrossRef]
78. Zachar, V.; Rasmussen, J.G.; Fink, T.; Zachar, V.; Pennisi, C.P.; Zachar, V.; Fink, T.; Gurevich, L.; Fojan, P. Isolation and growth of adipose tissue-derived stem cells. *Methods Mol. Biol.* **2011**, *698*, 243–251.